THE DEVELOPMENT OF A HIGH-THROUGHPUT AXISYMMETRIC ADHESION TEST

Aaron M. Forster[†], *Wenhua Zhang*[‡], *Christopher M. Stafford*[‡]
[‡]*Polymers Division, National Institute of Standards and Technology*
Gaithersburg, Maryland, 20899

current address:
[†]*U. S. Army Research Laboratory, Weapons & Materials Research Directorate*
Aberdeen Proving Ground, Maryland, 21005

Introduction

There has been a growing effort to extend combinatorial and high throughput (C&HT) methods into many aspects of material science, including material property screening and materials discovery. In material science, a prevalent approach to combinatorial library design is to incorporate continuous material property gradients across a specimen. Gradients provide convenient access to a large parameter space, tunable by the range and slope of property change along the sample.[1]

New toolsets are continually required to quantify material properties along these gradients. The multilens combinatorial adhesion test (MCAT) was created [2] to conduct parallel axisymmetric adhesion tests across gradient substrates. The MCAT technique utilizes an array of hemispherical lenses to conduct multiple axisymmetric adhesion tests during one loading/unloading cycle, see Figure 1.

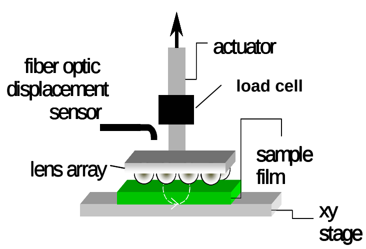

Figure 1: Schematic of the MCAT axisymmetric adhesion test geometry. Displacement is measured with a fiber optic displacement sensor and the contact area is viewed through the film.

The Johnson, Kendall, and Roberts (JKR) theory [3] describes the contact radius when two elastic hemispheres are brought together under load as a function of material properties and adhesion. The test is usually conducted by loading (compressing) and unloading (decompressing) two hemispheres against each other and measuring load, contact area, and displacement to provide a single adhesion measurement. This method may be applied in a serial manner for C&HT studies [4]; however a serial approach results in increased experimental time to completely characterize a combinatorial library. Parallel adhesion tests, using an array of lenses, produce multiple adhesion tests in a greater testing density than is possible with traditional single lens techniques.

The JKR theory is a modification of the Hertz equations of contact that takes into account the adhesive forces within the contact zone between two materials. The governing equations for this theory have been derived by several authors throughout the literature [5,6]. One challenge with the multilens test is the inability to quantify adhesion using load signals. In the current MCAT configuration, only the displacement of the lens array is measured along with contact area. This challenge may be overcome by the use of the overall lens array displacement rather than the load and requires one to derive the energy release rate in terms of displacement rather than load, as was shown by several authors [5].

$$\delta = \delta_O + \delta' - \sqrt{\frac{2\pi a \mathcal{G}}{E^*}} \qquad (1)$$

In equation (1), δ_0 is the displacement at initial contact between the lens and substrate, δ is the displacement, $\delta'=a^2R^{-1}$ is the hertzian displacement, a is the contact radius, $\mathcal{G}$ is the energy release rate or work of adhesion (loading), and E^* is the system modulus given by:

$$\frac{1}{E^*} = \frac{\left(1-\nu_L^2\right)}{E_L} + \frac{\left(1-\nu_S^2\right)}{E_S} \qquad (2)$$

where E_x and ν_x are modulus and Poisson's ratio for the substrate (S) and lens (L), respectively. From equation (1), we see that the displacement predicted for the adhesive case is always less than predicted by the Hertzian displacement.

The initial contact between the lens and substrate is not directly measured in an experiment. Uncertainty in the displacement at initial contact will also lead to uncertainty in the measured $\mathcal{G}$. Therefore, δ_0 and $\mathcal{G}$ are used as parameters to fit equation (1) to experimentally measured contact areas and the overall lens array displacement.

Utilizing the multilens array in conjunction with equation 1 is not straightforward because the displacement signal is much more sensitive to confinement than the corresponding load signal. Several questions remain about the ability of the multilens technique to accurately measure $\mathcal{G}$. We are concerned with how the lens size, test velocity, lens mechanical properties, and overall displacement affect the work of adhesion derived from the MCAT measurement.

Experimental

Materials

Two different multilens array geometries were used for adhesion tests. The first array is a square grid that is 3.25 cm^2 and contains 324 lenses. Each lens is 900 μm in diameter and 300 μm in height with a periodicity of 1000 μm and a radius of curvature of 500 μm (MicroFab Technologies). We only focus on 7 lenses for testing and do not discuss these tests due to abstract space constraints. The second array is composed of 4 individual glass lenses. Each lens in this array has a diameter of 3 mm and a height of 1.5 mm with a radius of curvature of 1.5 mm (ISP Optics). This abstract will focus on testing this array of 4 against a model glass substrate.

Measurements

For these experiments, negative lens arrays are replicated into Sylgard 184 (Dow Corning) polydimethylsiloxane (PDMS) from glass or epoxy master arrays using conventional casting techniques. A second batch of PDMS is used in a ratio of 10:1 prepolymer to catalyst to form a positive lens array from the negative mold and flat PDMS coupons ~2 mm thick. The PDMS is allowed to degas for several hours under vacuum and then cured at 70 ºC in a convection oven for 1 h. The sol fraction (uncrosslinked polymer) within the lenses is not extracted and the tensile modulus of the cured elastomer is 2.49 MPa ± 0.015 MPa. The replication process results in a 1 mm thick backing of PDMS capped with the lens array. The capping layer is believed to eliminate finite size effects from compression of the lenses. [5]

For these experiments, 50 mm x 75 mm borosilicate glass slides (Corning Glass Works) were cleaned with an excess of toluene, acetone, and ethanol (all from Aldrich). After drying with nitrogen gas, the slides were cleaned in a UVO chamber for 20 minutes and the solvent rinse was repeated. Finally, the slides were dried using nitrogen gas.

Adhesion tests were run as step tests, with time in between steps to capture contact area pictures. The size of the steps was changed from (1 to 3) μm to alter test velocity. The resultant velocities ranged from (0.056 to 0.095) μm/s.

Results and Discussion

For this extended abstract, two specific questions concerning the MCAT adhesion test will be addressed: Is the contact behavior (a vs. δ) influenced by total displacement? or whether the lens is soft or rigid? We first address the issue of total displacement.

An array of three identical PDMS lenses was brought into contact with a glass substrate. The test was conducted at a step size of 1 μm. Three separate loading/unloading cycles were conducted. The first cycle (δ_{max}=20 μm) contacted only one lens with the substrate. The second and third tests (δ_{max}=30 μm and 60 μm, respectively) contacted all three lenses with the substrate.

Figure 1 is the load versus displacement (P vs. δ) and contact radius versus displacement (a vs. δ) for the single lens in contact with a glass substrate. In both curves, the solid line represents the theoretical JKR-displacement fits. The contact radius data is shifted by δ_O in order to superimpose the theoretical and experimental curves on top of each other.

The system modulus was used as a fitting parameter (equation 3) to fit the load and displacement data in figure 1a. [6]

$$\delta_{JKR} = \frac{a^2}{R} + \frac{P}{2E^* a} \qquad (3)$$

where P is load, a is contact radius, and δ_{JKR} is the predicted displacement. Equation 3 is advantageous because it permits the determination of E^* without accounting for $\mathcal{G}$. The system modulus, E^*, was found to be 3.4 MPa, (E=2.55 MPa) which is comparable to the measured PDMS tensile modulus of E=2.49 MPa. After determining the system modulus, equation 1 was used to determine the work of adhesion and initial contact from the loading curve, $\mathcal{G}$=18 ± 5 mJ/m^2 and δ_O= 8 μm. It is apparent from the figure that the JKR fit to the loading data for a single lens acceptable and there is a small amount of hysteresis.

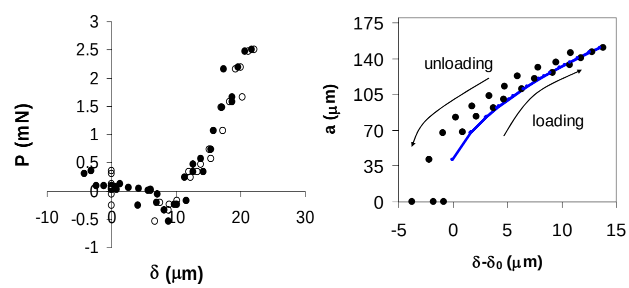

(a) (b)

Figure 2: a) P vs. δ for a single lens in contact with a glass slide. The theoretical fit (unfilled points) was calculated using equation 3. b) a vs. δ-δ_O for a single lens in contact with a glass slide. The theoretical fit (solid line) was calculated using equation 1.

Figure 3 is the contact radii versus displacement for the loading/unloading of three lenses against the glass substrate and δ_{max}=60 μm. Figure 3a shows the full loading/unloading cycle along with the JKR fits. The work of adhesion used to generate the line in the graph was $\mathcal{G}$=18 ± 5 mJ/m^2. The contact behavior of each lens is similar, but deviates significantly from JKR theory at contact radii greater than 150 μm. Figure 3b shows the contact behavior of the first and last lenses to contact the substrate and the previous single lens test superimposed over each other. It is evident from this graph that the loading/unloading paths are similar for these three lenses. We have observed the deviation from JKR theory at large compression for smaller lens arrays, but do not have a clear understanding of its origin at this time [7]. It is interesting to note that a reduction in the radius of curvature from 1.56 mm to 1.30 mm leads to an extremely good fit of the theoretical and experimental contact data (not shown).

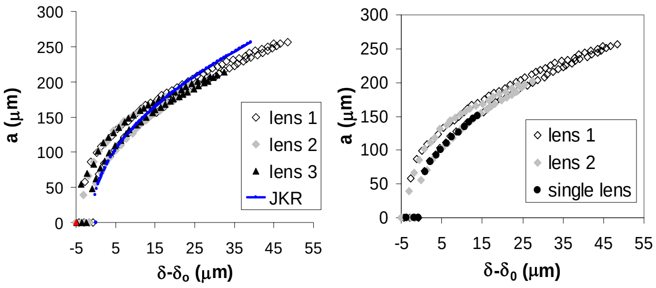

(a) (b)

Figure 3: a vs. δ for the multilens array. a) The symbols represent three lenses and the line is equation 1. b) a vs. δ for the first and last lens to contact the glass substrate. The data from the single lens experiment (δ_{max}=20 µm) has also been added.

In order to elucidate further the effects of the multilens array on the individual lens contact behavior of each lens, we switched the materials. We now address the issue of whether lens material is influential in a multilens test. Quartz lenses of the same dimensions as the previous PDMS lenses were tested against the coupon of PDMS made at the same time as the PDMS lenses. Figure 3 shows the contact radius versus displacement for this test with δ_{max}= 45 µm. Note this test was conducted as a step test with 3 µm steps. The JKR equation was again fit using $\mathcal{G}$=18 ± 5 mJ/m^2. This is the same value used for the PDMS lenses against the glass slide. There are several important features in this figure. The first is the similar

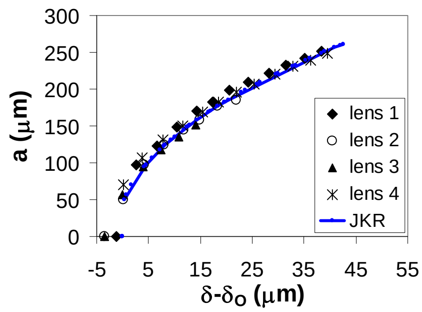

Figure 4: a vs. δ for a glass lens array of four lenses. The solid line is the JKR fit, equation 1.

contact behavior between the different lenses. The second is the lack of hysteresis between the loading and unloading curves. Finally, the experimental data do not deviate from the JKR fit at large contact areas.

Summary and Conclusions

The ability to model contact behavior using the displacement form of the JKR equation demonstrates that the multilens technique measures the work of adhesion simultaneously at multiple contact points. Similar values of the work of adhesion were obtained for both soft and rigid hemispheres. This technique is not perfect because the overall displacement of the lens array is measured rather than the displacement of individual lenses. Therefore, compliance of the backing layer can not be measured. Also, a displacement based measurement will not replace the load based JKR equations in terms of accuracy.

The use of soft, elastic lens arrays remains a challenge. The source of deviations from JKR theory in contact behavior above a threshold contact radius is not clear at this time. The lack of deviations for rigid hemispheres suggests that the multilens array is not necessarily the source of deviations. It is possible the geometry of the soft lens array confines the lenses below equilibrium contact area and this will be one subject of the presentation.

ACKNOWLEDGEMENTS

AMF acknowledges Dr. Peter Drzal and Dr. Arnaud Chiche (NIST) for helpful discussions. AMF acknowledges Dr. Roman Koetitz (Rhodia, Inc.) for image analysis assistance. AMF and CMS acknowledge the National Research Council Postdoctoral Fellowship program for financial support.

‡ Certain commercial equipment and materials are identified in this paper in order to specify adequately the experimental procedure. In no case does such identification imply recommendations by the Army Research Lab nor does it imply that the material or equipment identified is necessarily the best available for this purpose.

REFERENCES

1. Smith, A. P.; Douglas, J. F.; Meredith, J. C.; Amis, E. J.; Karim, A. *Physical Review Letters* 2001, **87**, 1-4.
2. Crosby, A. J.; Karim, A.; Amis, E. J. *Journal of Polymer Science Part B-Polymer Physics* 2003, **41**, 883-891.
3. Johnson, K. L.; Kendall, K.; Roberts, A. D. *Proceedings of the Royal Society of London A: Materials* 1971, **324**, 301.
4. Grunlan, J.C., Holguin, D.L., Chuang, H.K., Perez, I., Chavira, A., Quilatan, R., Akhave, J., Mehrabi, A.R., *Macromolecular Rapid* Communications, 2004, **25**, 286-291.
5. Deruelle, M.; Hervet, H.; Jandeau, G.; Leger, L. *Journal of Adhesion Science and Technology* 1998, **12**, 225-247.
6. Shull, K. R. *Materials Science & Engineering R-Reports* 2002, **36**, 1-45.
7. Forster, A.M., Zhang, W., Stafford, C.M., accepted *Measurements Science and Technology*.